https://doi.org/10.5194/amt-2023-11
Preprint. Discussion started: 8 March 2023

Atmospheric Measurement Techniques Discussions

First-time comparison between NO_2 vertical columns from GEMS and Pandora measurements

Serin Kim[1], Daewon Kim[1], Hyunkee Hong[2], Lim-Seok Chang[2], Hanlim Lee[1], Deok-Rae Kim[2], Donghee Kim[2], Jeong-Ah Yu[2], Dongwon Lee[2], Ukkyo Jeong[1], Chang-Kuen Song[3], Sang-Woo Kim[4], Sang Seo Park[3], Jhoon Kim[5], Thomas F. Hanisco[6], Junsung Park[1], Wonei Choi[1], Kwangyul Lee[7]

[1]Division of Earth Environmental System Science, Major of Spatial Information Engineering, Pukyong National University, Busan, Republic of Korea
[2]Environmental Satellite Center, National Institute of Environmental Research, Incheon, Republic of Korea
[3]Department of Urban & Environmental Engineering, Ulsan National Institute of Science and Technology, Ulsan, Republic of Korea
[4]School of Earth and Environmental Sciences, Seoul National University, Seoul, Republic of Korea
[5]Department of Atmospheric Sciences, Yonsei University, Seoul, Republic of Korea
[6]Atmospheric Chemistry and Dynamics Lab, NASA Goddard Space Flight Center, Greenbelt, MD, USA
[7]Air Quality Research Division, Climate and Air Quality Research Department, National Institute of Environmental Research, Incheon, Republic of Korea

Correspondence to: Daewon Kim (k.daewon91@gmail.com)

Abstract. The Geostationary Environmental Monitoring Spectrometer (GEMS) is a UV–visible spectrometer onboard the GEO-KOMPSAT-2B satellite launched into geostationary orbit in February 2020. To evaluate GEMS NO_2 column data, comparison was carried out using NO_2 vertical column density (VCD) measured using direct-sunlight observations by the Pandora spectrometer system at four sites in Seosan, South Korea, during November 2020 to January 2021. Correlation coefficients between GEMS and Pandora NO_2 data at four sites ranged from 0.35 to 0.48, with root mean square errors (RMSEs) from 4.7×10^{15} molec. cm^{-2} to 5.5×10^{15} molec. cm^{-2} for cloud fraction (CF) < 0.7. Higher correlation coefficients of 0.62–0.78 with lower RMSEs from 3.3×10^{15} molec. cm^{-2} to 4.3×10^{15} molec. cm^{-2} were found with CF < 0.3, indicating the higher sensitivity of GEMS to atmospheric NO_2 in less-cloudy conditions. Overall, GEMS NO_2 column data tend to be lower than those of Pandora due to differences in representative spatial coverage, with a large negative bias under high-CF conditions. With correction for horizontal representativeness in Pandora measurement coverage, the correlation coefficients range from 0.69 to 0.81 with RMSEs from 3.2×10^{15} molec. cm^{-2} to 4.9×10^{15} molec. cm^{-2} were achieved for CF < 0.3, showing the better correlation with the correction than that without the correction.

1 Introduction

Nitrogen dioxide (NO_2) is a key species in the troposphere and stratosphere for atmospheric chemistry and air quality (Crutzen, 1979; Seinfeld and Pandis, 1998), which is mainly emitted by anthropogenic sources such as fossil fuel combustion in vehicles and plants. Natural sources such as lightning, biomass burning, and soil microbial action are also major contributors to atmospheric NO_2 (Crutzen, 1979). NO_2 is precursor of tropospheric ozone, aerosol, and the hydroxyl radical (OH) (Boersma et al., 2009), and high concentrations affect the lifetime of atmospheric CH_4 and direct radiative forcing of the atmosphere (Pinardi et al., 2020).

Therefore, it is important to monitor NO_2, and representative methods for this are as follows. Chemiluminescence-based in-situ instruments have provided a highly accurate NO_2 mixing ratio at a measurement location, but with limited spatial coverage (e.g., Bechle et al., 2013; Jeong and Hong, 2021). Satellite-based remote sensing instruments on polar orbits, such as the GOME-1/2 (Global Ozone Monitoring Experiment; Burrows et al., 1999; Munro et al., 2016), SCIAMACHY (Scanning Imaging Spectrometer for Atmospheric Cartography; Bovensmann et al., 1999), OMI (Ozone Monitoring Experiment; Levelt et al., 2006), and TROPOMI (TROPOspheric Monitoring Instrument; Veefkind et al. 2012), have effectively complemented the ground-based observations by providing global distribution of NO_2 total column density (Lamsal et al., 2014). The recently launched GEMS (Geostationary Environment Monitoring Spectrometer; Kim et al., 2020) onboard the GEO-KOMPSAT-2B (Geostationary Korea Multi-Purpose Satellite 2B) provides diurnal variations of the NO_2 VCD during daytime over Asia since February 2020. The NIER (National Institute of Environment Research), where the GEMS ground station is operated, has been transmitting the GEMS products including NO_2 column in real time from December 2022. GEMS Map of the Air Pollution (GMAP) campaigns have taken place from 2020 and are also scheduled to be held annually to evaluate the quality of the GEMS by the measurements of trace gas and aerosol products based on trace gases, aerosol composition and optical property measurements at various platforms. This study conducted the first quick evaluation via comparison between the GEMS NO_2 column data and those of Pandora measurements at several sites in a suburban area in Korea during the first GMAP campaign in 2020 winter. We evaluate the differences between NO_2 VCD obtained from Pandora and GEMS especially depending on cloudy and clear sky conditions.

Comparison and validation of the satellite-based NO_2 VCD retrievals are essential due to their non-negligible error sources such as assumed atmospheric profile, surface reflectance, and measurement uncertainties (Hong et al., 2017). In addition, the diurnal NO_2 VCD retrievals from the GEMS require precise assessments as the observation geometries of the geostationary Earth orbit (GEO) are different from those of the low earth orbits (LEO) and other systematic uncertainties may affect the retrievals (e.g., diurnal variations of the atmospheric profiles, which are used for the air mass factor (AMF) calculations). Ground-based remote sensing instruments such as the MAX-DOAS (multi-axis differential optical absorption spectroscopy; Honninger et al., 2004) measures scattered sunlight at various elevation angles to derive tropospheric column amounts of NO_2 as well as the profile estimates (e.g., Irie et al., 2008; Wagner et al., 2011; Wang et al., 2017). Direct-Sun instruments such as the Pandora (Herman et al., 2009) measure direct sunlight to retrieval NO_2 VCD, of which the absorption light path of the photons reaching to their detector may be shorter than those of the MAX-DOAS instruments, thus less sensitive to the surface mixing ratio of the NO_2. However, NO_2 VCD retrievals from the Pandora and direct-sun DOAS have lower uncertainty of the AMF calculations as they utilize simple geometric AMF, whereas that for the MAX-DOAS algorithms take into account the atmospheric profiles as well as the Raman scattering (Herman et al., 2009). Numerous studies have utilized the recently expanding global network of Pandora (PGN; https://www.pandonia-global-network.org/) for validation of comparison of the

https://doi.org/10.5194/amt-2023-11
Preprint. Discussion started: 8 March 2023

polar-orbiting satellite products (e.g., Herman et al., 2009; Tzortziou et al., 2014, 2015; Herman et al., 2019; Judd et al., 2019, 2020; Pinardi et al., 2020; Verhoelst et al., 2021).

This study represents the first attempt to compare and validate NO_2 VCD retrievals from the GEMS with the Pandoras deployed during the GMAP (GEMS Map of the Air Pollution; from November 2020 to January 2021) campaign around Seosan, South Korea. Seosan is a sub-urban area, and while the second campaign compared and validated at multiple sites from mega-city to sub-urban characteristics using Pandora and MAX-DOAS after this campaign. The measurement periods and locations of the four Pandora instruments used in this study are summarized in Figure 1 and Table 1. In Section 2, the explanation of campaign and used GEMS data are described, followed by the Pandora instrument and retrieval methodology. Section 3 provides a method of comparison between instruments and between Pandora and GEMS. Results are described in three parts in Section 4: intercomparison between Pandora instruments, the results of comparison with GEMS NO_2, and considering horizontal representativeness. Finally, the conclusions are provided in Section 5.

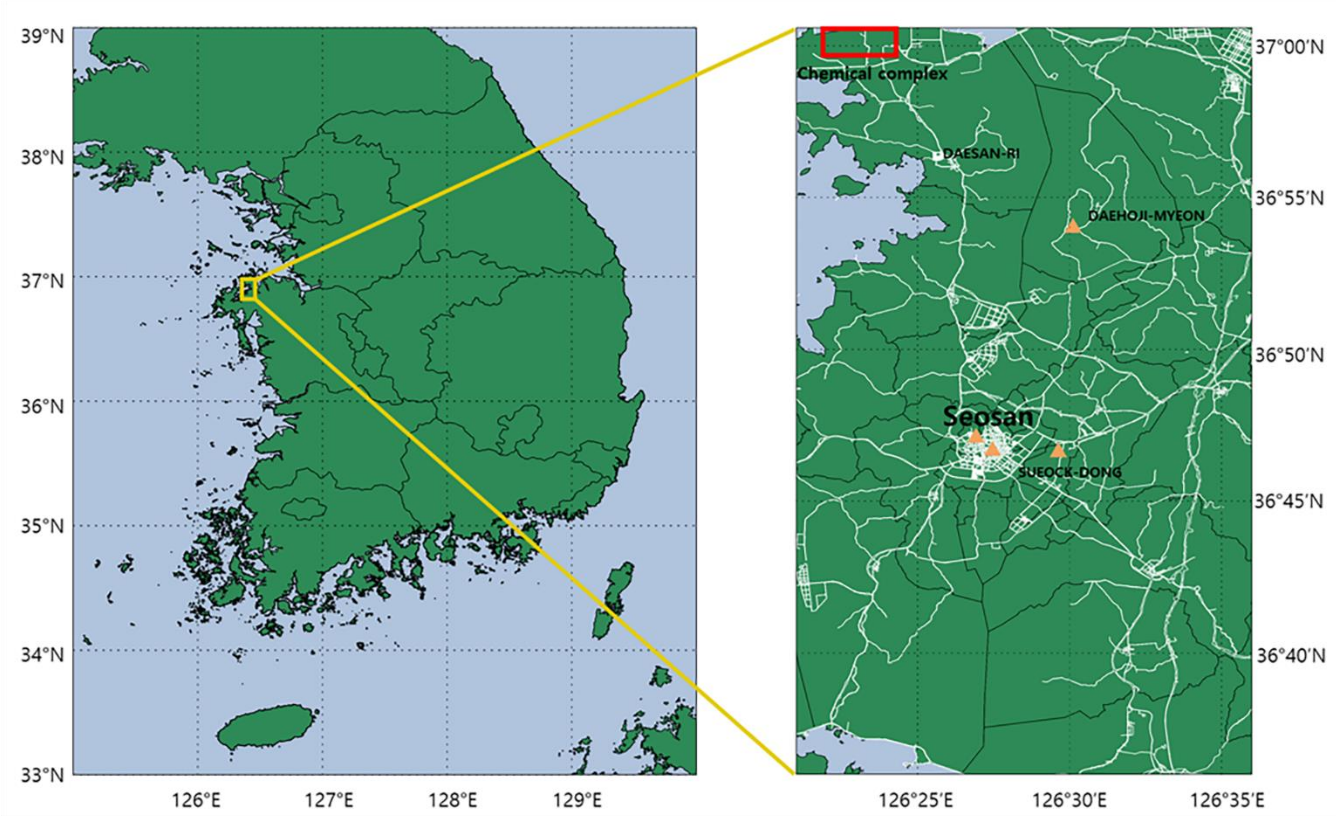

Figure 1. Measurement sites for the GMAP 2020 campaign. Triangles indicate observation sites

https://doi.org/10.5194/amt-2023-11
Preprint. Discussion started: 8 March 2023

Atmospheric Measurement Techniques Discussions

Table 1. The information of measurement sites and period.

	Latitude	Longitude	period
Seosan (SS)	36.78° N	126.49° E	2020.11.12–2020.12.03 2020.12.03–2021.01.27
Seosan-CC (CC)	36.78° N	126.45° E	2020.12.09–2021.01.31
Daehoji (DHJ)	36.90° N	126.50° E	2020.12.09–2021.01.17
Dongmoon-2dong (DM2)	36.78° N	126.46° E	2020.12.09 – 2021.01.03

2 GMAP campaign

2.1 The first GMAP campaign

GMAP 2020, the first GEMS validation campaign, was conducted during November 2020 to January 2021 in Seosan city. Pandora instruments used in the campaign were of the standard version described in Section. 3.1. The mean NO_2 concentration at Seosan for 2016–2020 was 0.017 ppm, ~0.16% lower than the Korean national five-year average (https://www.airkorea.or.kr/web, last access: 07 March 2021). Measurements of direct sunlight were carried out at four sites, as described in Table 1 and Fig.1: Seosan (SS), Seosan City Council (CC), Dongmun-2dong (DM2), and Daehoji (DHJ). Emissions from vehicular and point sources may have contributed to variations in NO_2 concentrations in Pandora lines of sight, depending on wind direction. Major roads and an agricultural complex are located within ~0.7 km of the SS site; a road and roundabout are near the CC site; a road is near the DM2 site; and a petrochemical complex is located ~16 km NW of the DHJ site. To estimate differences in NO_2 VCD among the Pandora instruments, an initial intercomparison was conducted for two weeks at the SS site. It needs to be noted that Pandora instruments were manufactured by the same optics and spectrograph. However, it is still important to quantify the differences between NO_2 columns retrieved from the four Pandoras at a same location before we compare with GEMS NO_2. From December 2020 to January 2021, the instruments were installed at the above four sites for the measurement of direct sunlight. Measurement periods varied owing to instrument conditions (Table 1).

2.2 GEMS NO_2 data

The GEMS, a hyperspectral UV-Vis image spectrometer covers a wavelength range of 300–500 nm with a full width half at maximum (FWHM) of about 0.6 nm measures atmospheric concentrations of species that affect air quality, such as NO_2, O_3, SO_2, HCHO, and aerosols on an hourly basis from 00:45 to 05:45 UTC with a spatial resolution of 3.5 × 8 km (Kim et al., 2020). GEMS NO_2 column retrieval is based on the DOAS algorithm (Platt and Stutz, 2008) at wavelength intervals of 432–

https://doi.org/10.5194/amt-2023-11
Preprint. Discussion started: 8 March 2023

Atmospheric Measurement Techniques Discussions

450 nm (Park et al., 2020). For the purpose of the data evaluation, we used GEMS L2 NO_2 VCD version 1.0, which were available immediately after the IOT (in Orbit Test) carried out in July in 2020.

2.3 Pandora Instrument and Spectral Fitting

Pandora is ground-based spectrometer which measures direct sunlight over the wavelength range of 280 nm to 525 nm with FWHM of about 0.6 nm. The Charge-coupled device (CCD) detector, which is equipped in the Pandora spectrometer consists of 2048×64 pixels. The spectrometer is connected to a telescope so called "head sensor" consisting of a collimator and filters such as UV340 filter, neutral density filters, and opaque filter through an optical fiber with a 400 µm core diameter. A target area can be observed with a field of view (FOV) of up to 1.6° (Herman et al., 2018).

The four instruments used here are referred to as P1, P2, P3, and P4. The measured spectra were analysed to retrieve NO_2 slant column densities (SCD) using QDOAS software (Fayt et al., 2011) based on DOAS technique. During the intercomparison, the radiance obtained at the noon time of November 28 (a clear day) was used as the reference spectrum for P1, P3, and P4. Here, a reference spectrum denotes a spectrum with least amount of NO_2 presence to carry out optical density fitting during a certain period. November 14 was used as a reference for P2 due to the lack of data on the 28th. As NO_2 differential VCD (dVCD) from P2 were retrieved using different reference spectrum, they were considered secondary data. NO_2 differential slant column density (dSCD) was obtained using the absorption cross-sections for NO_2 254.5K generated using 220K and 294K (Vandaele et al., 1998) and O_3 225K (Serdyuchenko et al., 2014), as a fourth-order polynomial in fitting window of 400-440 nm. The wavelength range and absorption cross-section were the same as those used in Pandonia Global Network (PGN) (https://pandora.gsfc.nasa.gov/, last access: 28 March 2022). We additionally used O_4 293K (Thalman and Volkamer, 2013) for the spectral fitting. This reduced retrieval errors by about 0.2 %. Figure 3 presents a deconvolution of the P1 spectral fitting at 10:43 Local Time (LT) on November 28, 2020. NO_2 VCD is obtained by dividing the NO_2 SCDs by geometric AMFs. After the initial intercomparison period, the reference spectrum was selected when the weather is clear with no air pollution, as instrument locations were different. P1 and P4 used noon spectrum on January 14, 2021, as a reference spectrum, whereas P2 and P3 used spectra from December 19, 2020.

Atmospheric Measurement Techniques Discussions

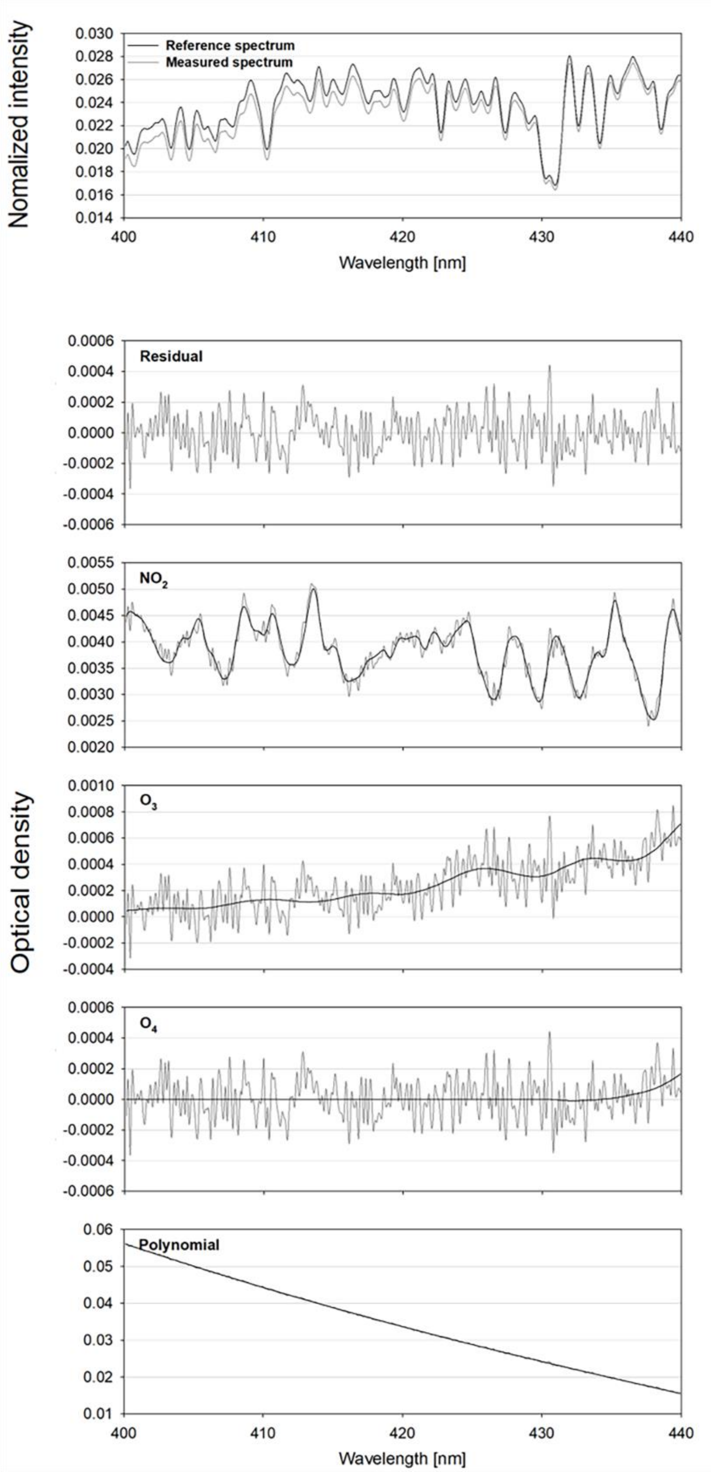

130 **Figure 2.** A deconvolution example for November 28 2020 at 10:43:37 LT for P1. The black line represents the absorption signal, and grey line represents the absorption signal and fit residual.

https://doi.org/10.5194/amt-2023-11
Preprint. Discussion started: 8 March 2023

Atmospheric Measurement Techniques Discussions

3 Method

The purpose of this study is to evaluate the GEMS NO_2 column data via quick comparisons between the GEMS NO_2 column data and those of Pandora measurements. The differences between the Pandora and GEMS NO_2 data can attribute to the uncertainties of Pandora and GEMS NO_2 column and differences in the measurement geometries. The spatiotemporal differences between Pandora and GEMS measurements also cause differences between the NO_2 column data obtained from those two different platforms. Differences between the Pandora NO_2 retrievals partially reflects the uncertainties of Pandora NO_2 column data. In order to quantify the differences of the Pandora NO_2 measurements, all four Pandoras performed the identical direct Sun measurements at the SS site during the intercomparison period by setting the same observation schedules for the all instruments. The specifications and retrieval methods of Pandora are described in Sect. 2.3. Since it measures direct sunlight, it is negligibly affected by the scattered sunlight. However, in cloudy conditions, all Pandora may not see the same location of Sun due to an inhomogeneity of cloud thinness. In thick cloudy conditions compared with those of clear sky, Pandora increases an exposure time to acquire strong enough radiance intensities, which may lead to the inclusion of unwanted stray light and increase detector noise. In order to understand the influence of the cloud, Pandora was investigated to see whether the signal was affected or not from clouds using GEMS cloud fraction (CF).

4 Results

4.1 The intercomparison of NO_2 dVCD from Pandora

The Pandora intercomparison was carried out during 12 November to 3 December, 2020, at the SS site to quantity NO_2 differential VCD (dVCD) retrievals from the Pandora instruments. We defined dVCD as the differential SCD divided AMFg with no background correction.

https://doi.org/10.5194/amt-2023-11
Preprint. Discussion started: 8 March 2023

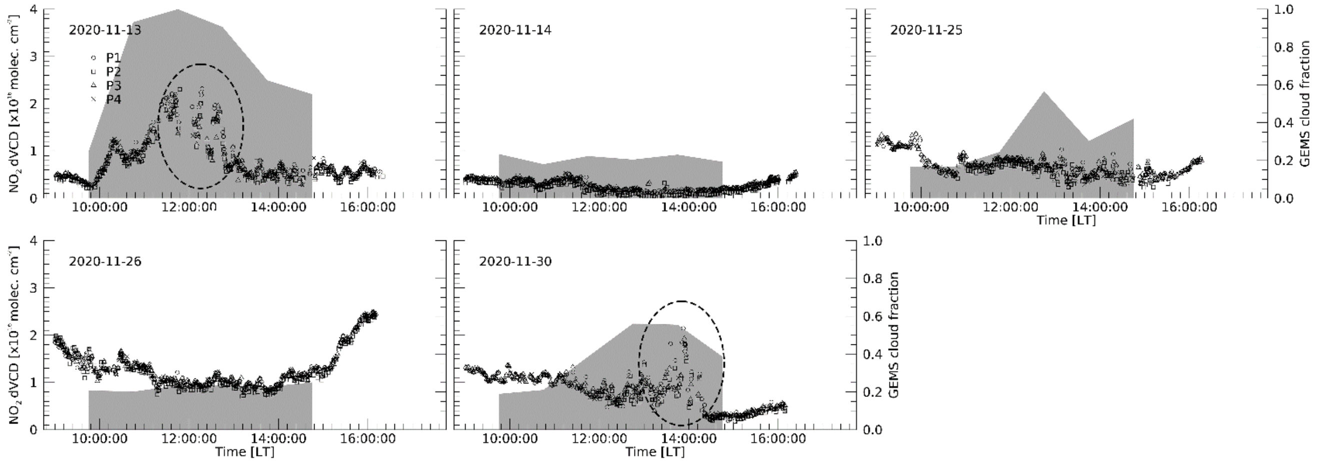

Figure 3. Time series of Pandora retrievals during the intercomparison. Circle, square, triangle and X symbols represent total NO_2 dVCD for P1, P2, P3, and P4, respectively. Grey shade represents the GEMS cloud fraction.

Time series of data from all instruments for the intercomparison period are shown in Fig. 3, except for rainy days. The circles, squares, triangles, and X symbols represent the NO_2 dVCD retrieved by P1, P2, P3, and P4, respectively, and the grey area represents the CF of the GEMS observation time (Fig. 3). The diurnal pattern of NO_2 between each Pandora showed good agreement. The NO_2 VCD during the period ranged from 1.63×10^{14} molec. cm^{-2} to 2.49×10^{16} molec. cm^{-2}, tend to increase during the morning and late afternoon (after 16:00). The dashed-line ovals (Fig. 3) indicate periods with discrepancies between Pandora instruments during the afternoons on November 13 and 30, likely due to cloud effects, as GEMS CFs were > 0.3 at the time. It is considered that the cloud contributed to the discrepancies since the GEMS CFs were higher than 0.3 on the dates with the discrepancies, which shows certain cloud effects on the NO_2 retrievals from the ground-based direct Sun measurements. Thus, we have carried out the comparisons between the NO_2 VCDs from Pandora and those from GEMS depending on the CF conditions less than 0.3, 0.5, and 0.7, respectively. Figure 5 shows the linear regression of the NO_2 dVCDs from P2, P3, and P4 against those from P1 during the intercomparison period, which produced least fitting errors in average during the intercomparison period.

https://doi.org/10.5194/amt-2023-11
Preprint. Discussion started: 8 March 2023

Atmospheric Measurement Techniques
Discussions

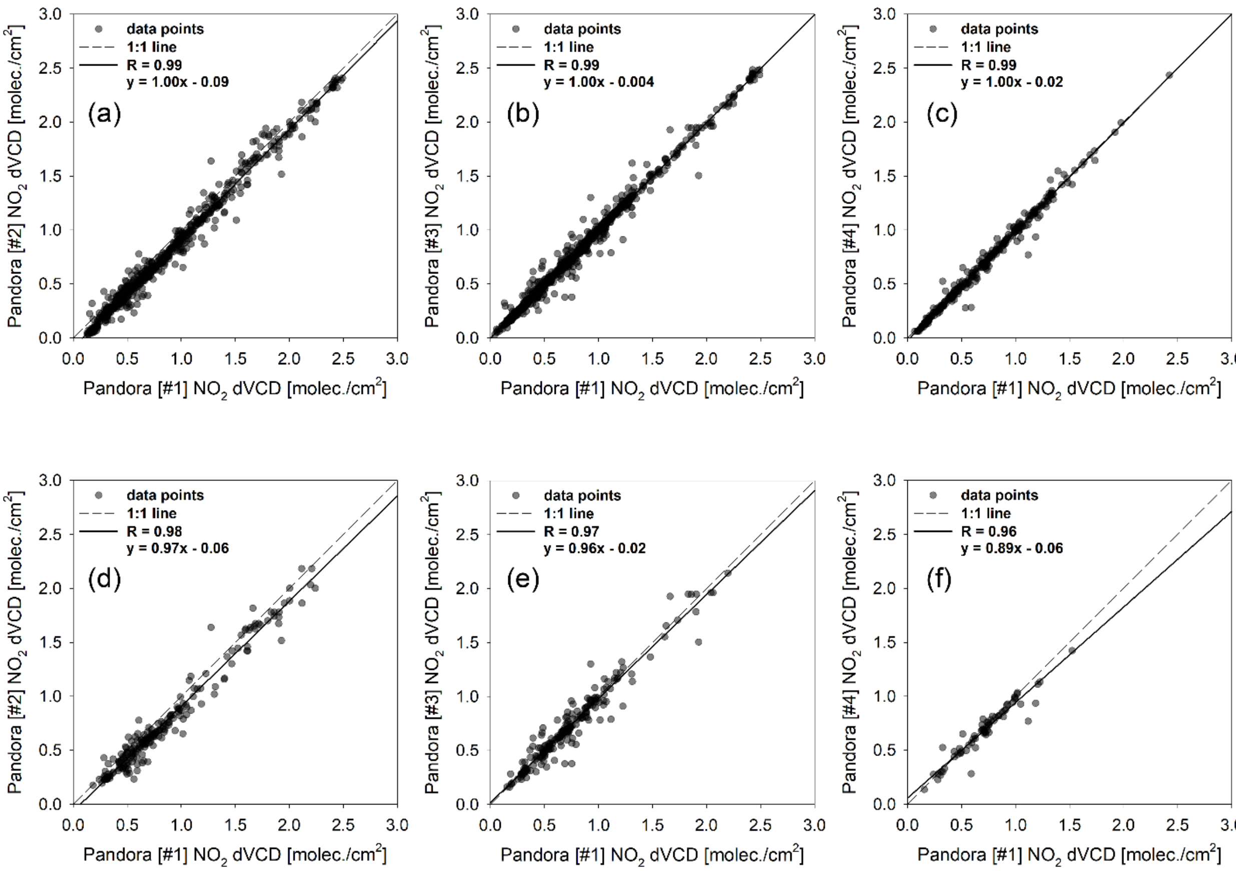

Figure 4. The scatter plots between P1 and others. (a), (b) and (c) shows comparison with all data of P2, P3 and P4. (d), (e) and (f) shows comparison with P2, P3 and P4 when GEMS CF > 0.3.

In Figure 4 a, b, and c, the correlation coefficients were found to be 0.99 with the slope of 1 and the interceptor between 0.004–0.09, showing the good agreement for all CF conditions. Overall, the NO_2 retrieved by each instrument yielded similar correlations, even with CF > 0.3, although R values were slightly lower in Fig. 4 d–f, with slopes deviating further from the 1:1 line.

4.2 Comparison of NO_2 VCD between Pandora and GEMS

After the intercomparison period, the Pandora instruments were moved to the four sites for the observation of direct sunlight to evaluate NO_2 VCD for comparison with GEMS data. Measurement was carried out from December 9, 2020, and it was either snowing or raining for more than half of the measurement period. For the validation of GEMS, Pandora data were averaged within ±10 minutes from the center of the GEMS observation time. GEMS measurement pixels are not fixed but rather change as a function of time. Therefore, comparisons were performed at each Pandora location with the GEMS pixels closet GEMS pixels. The comparisons are carried between the NO_2 VCDs obtained from Pandora and GEMS depending on the CFs of 0.3, 0.5, and 0.7, respectively. Direct-sun DOAS (DS-DOAS) horizontal absorption path lengths are generally within 4 km, with solar zenith angle (SZA) < 50° (Herman et al., 2009). However, most the SZAs were larger than 50° during the campaign period. Thus, the single GEMS pixel sometimes may not cover the absorption path of the Pandora observation. This horizontal discrepancy was partly considered for the comparison between Pandora NO_2 data and those of GEMS, which can be found in the Section 4.3.

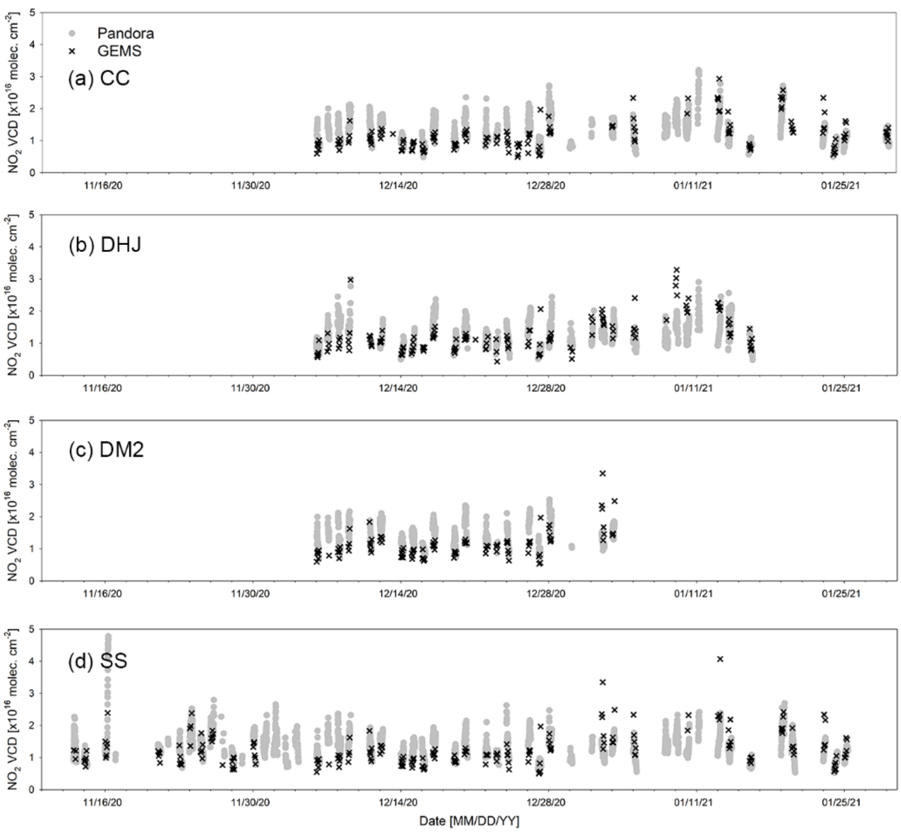

Figure 5. Hourly variations in NO_2 VCD obtained from Pandora (grey full circles) and GEMS (black **x**). (a), (b), (c), and (d) represent the CC, DHJ, DM2, and SS sites, respectively.

https://doi.org/10.5194/amt-2023-11
Preprint. Discussion started: 8 March 2023

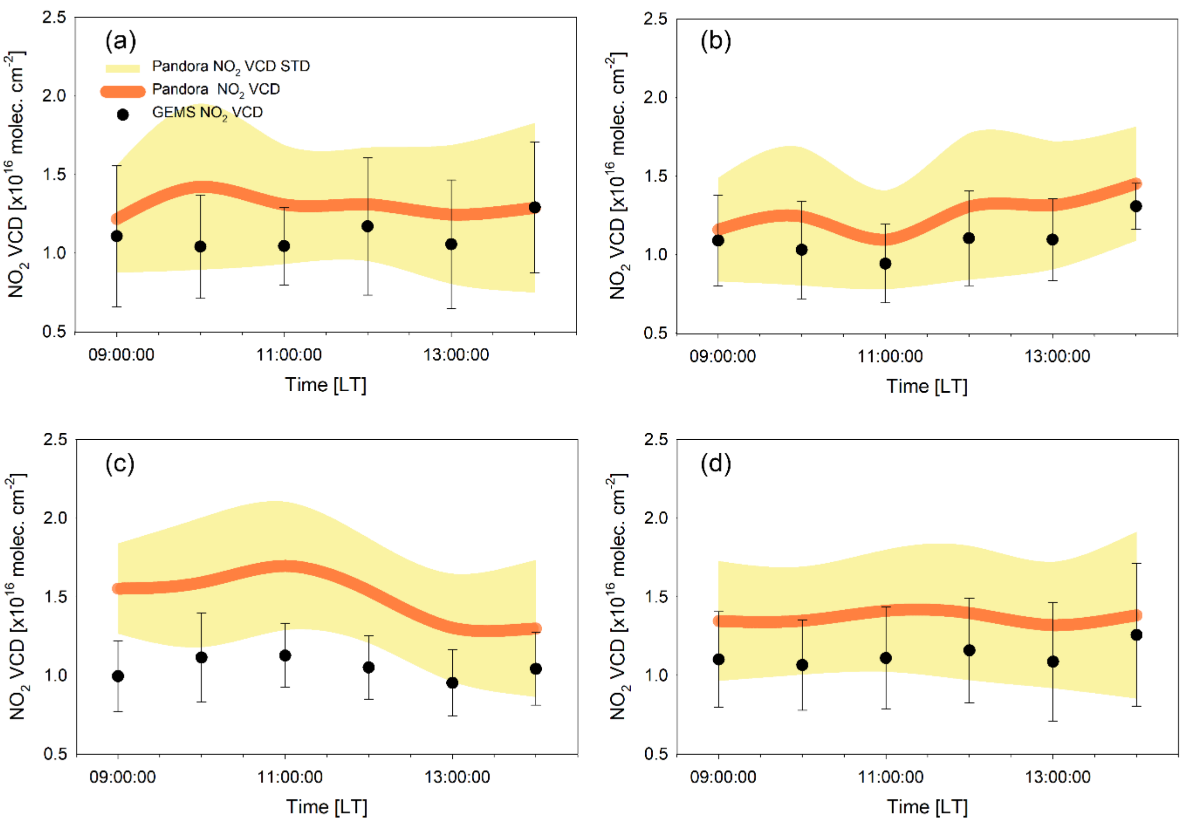

Figure 6. Hourly mean NO_2 VCD from Pandora (orange line) and GEMS (black solid circles). (a), (b), (c), and (d) represent the CC, DHJ, DM2, and SS sites, respectively. Yellow shading represents the standard deviations of Pandora NO_2 VCD, and bars show those of GEMS; STD = standard deviation.

Daily variations NO_2 VCD obtained from Pandora and GEMS are illustrated in Fig. 5 and compared for each of the four Seosan sites in Figure 6. Differences in diurnal Pandora NO_2 VCD variations among the sites imply inhomogeneity of spatial tropospheric NO_2 columns over the sites. The hourly characteristics observed at the DHJ site could be affected possibly by emissions from the petrochemical complex located about 16 km in a north westerly direction from the site (see Fig. 1). It seems that there is a discrepancy in the NO_2 peaks observed from Pandora and GEMS at the CC site where GEMS shows the enhanced NO_2 columns at 12:00 and 14:00 LT. The NO_2 columns observed from GEMS are found to show their hourly patterns similar to those from Pandora at the DHJ site. At the DM2 site, we found a good agreement between the NO_2 columns observed from Pandora and GEMS. At the DM2 site, Pandora and GEMS VCD patterns were consistent, with both displaying peaks at 11:00 LT followed by a decreasing trend. Overall, NO_2 VCD from Pandora and GEMS show negligible hourly variations, although those of Pandora tended to have slightly higher values than those of GEMS. There could be several reasons for this difference,

https://doi.org/10.5194/amt-2023-11
Preprint. Discussion started: 8 March 2023

as discussed later. Further quantitative comparisons on Pandora and GEMS data were carried out, as discussed below. In order to understand the correlation between Pandora and GEMS, the quantitative comparison was further performed.

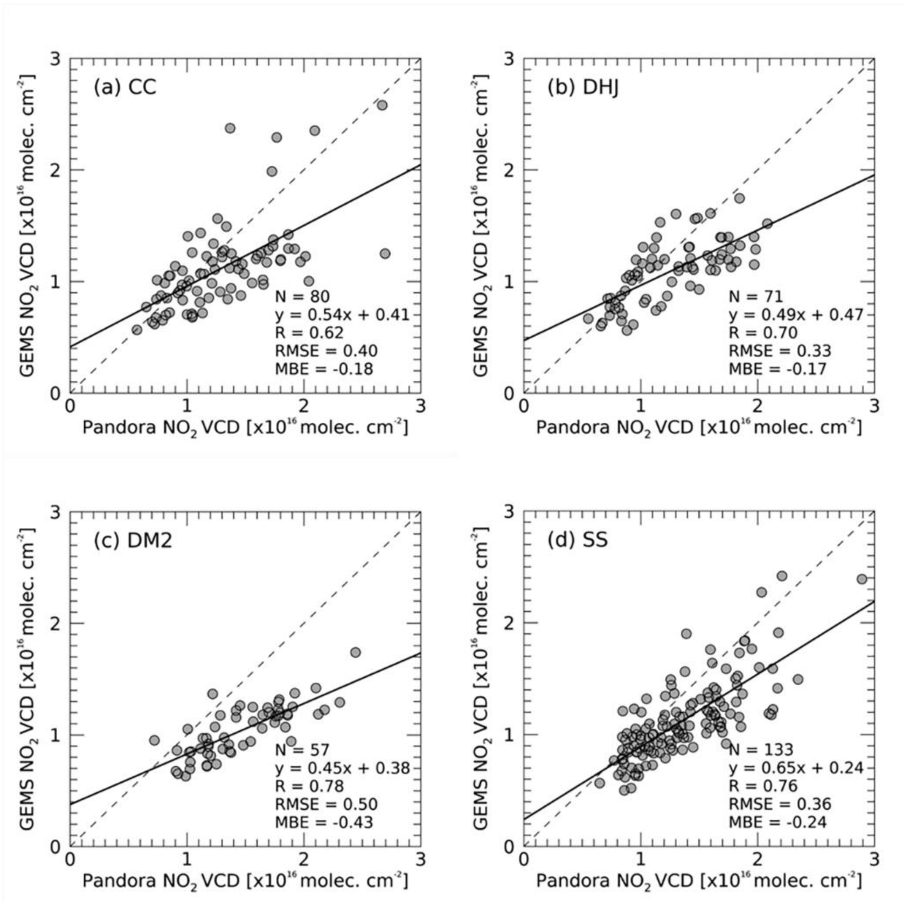

Figure 7. The scatterplot of NO_2 VCD between Pandora and GEMS in the CF < 0.3. (a), (b), (c) and (d) represent the CC, DHJ, DM2, and SS site, respectively. The grey dashed line represents the 1:1 line and the black solid line represents the regression line.

Figure 7 shows the correlations between NO_2 VCD for the Pandora and GEMS measurements at the four Seosan sites are shown in Fig. 8 for CF of < 0.3. The R values are range from 0.60 and 0.78, with values of 0.62, 0.70, 0.78, and 0.76 at the CC, DHJ, DM2, and SS sites and slopes of 0.54, 0.49, 045, and 0.65, respectively. Although these comparisons were conducted over a short time period, NO_2 VCD retrieved from the geostationary GEMS measurements shows good correlations with those observed from ground-based Pandora measurement sites. The root mean square errors (RMSE) of the GEMS NO_2 against Pandora were 0.40, 0.33, 0.50, and 0.36 at the CC, DHJ, DM2, and SS sites, while mean bias errors are -0.18, -0.17, -0.43 and -0.24, respectively

https://doi.org/10.5194/amt-2023-11
Preprint. Discussion started: 8 March 2023

Atmospheric Measurement Techniques Discussions

In this study, the TROPOMI NO_2 total columns of the offline channel (OFFL) dataset with a quality assurance (QA) value larger than 0.75 and a Cloud radiance fraction less than 0.3 used and compared with Pandora NO_2. The correlation coefficients between NO_2 total column from Pandora and TROPOMI are range from 0.58 to 0.74. For the CC, DHJ, DM2 and SS sites, RMSE of the TROPOMI NO_2 against Pandora are calculated 0.51, 0.38, 0.70, and 0.52 and MBE are -0.42, -0.19, -0.64, and -0.46, respectively. In the case of GEMS, the RMSE was slightly smaller than that of TROPOMI, and there was a tendency to underestimate less.

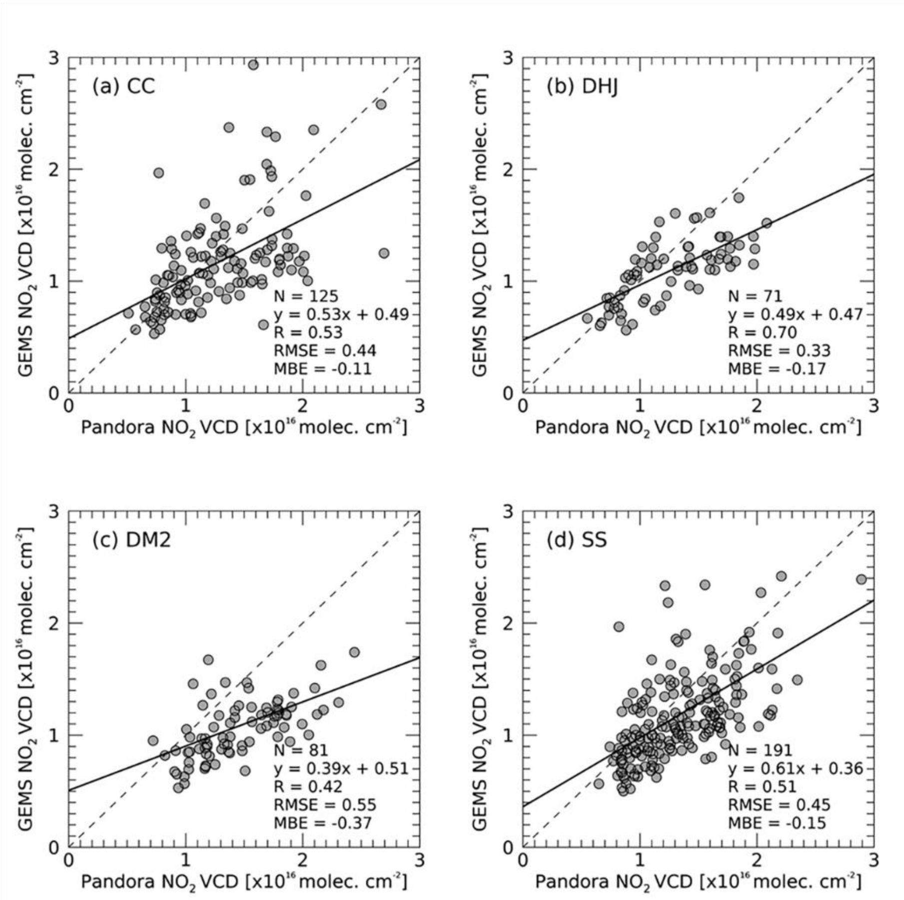

Figure 8. The scatterplot of NO_2 VCD between Pandora and GEMS in the CF conditions < 0.5 (a), (b), (c) and (d) represent the CC, DHJ, DM2, and SS site, respectively. The grey dashed line represents the 1:1 line and the black solid line represents the regression line.

Figure 8 and 9 shows the correlations between NO_2 VCD obtained from Pandora and GEMS measurements with the CF < 0.5 and < 0.7, respectively. R values tends to decrease with the increasing CF value and are in the ranges of 0.42–0.53 for CF < 0.5 and 0.35–0.48 for CF < 0.7, with slopes of 0.53, 0.55, 0.39, and 0.62 and 0.54, 0.62, 0.38, and 0.62 at the CC, DHJ, DM2, and SS sites, respectively. The RMSE of the GEMS NO_2 VCD against Pandora NO_2 values tends to increase with high CF

https://doi.org/10.5194/amt-2023-11
Preprint. Discussion started: 8 March 2023

Atmospheric Measurement Techniques Discussions

value and the correlation coefficient decreases (Fig. 10). High correlation coefficient and low RMSE in the low CF conditions indicate that the diurnal NO_2 variations observed by GEMS are consistent with those of Pandora in less cloudy conditions. The tendency of correlation coefficient and RMSE against the variations of the CF conditions implies that the enhanced cloud condition may degrade the sensitivity of the GEMS measurement to NO_2 molecules present below or at the cloud layers. However, given the discrepancies among the NO_2 VCD from four Pandora instruments at the same SS location, especially in cloudy conditions (CF$>$0.3; Fig. 4), the weaker correlations between the GEMS and Pandora data at higher CF conditions may be partly due to the uncertainties in Pandora NO_2 VCD at high CF.

Variations of MBE with CF are illustrated in Fig. 10, showing that the negative bias of GEMS against Pandora generally decreases with increasing CF. Indeed, a positive bias was observed at the DHJ site with the CF < 0.7. Except for the DM2 site, the magnitudes of negative bias in the high CF value (< 0.7) are quite small in comparison with CF < 0.3. Increasing negative bias in GEMS NO_2 against that of Pandora could be associated with the GEMS CF, which are used to calculate the GEMS NO_2 AMF. Regarding the Pandora NO_2 VCD as being closer to the true values than those of GEMS, the large negative bias of the GEMS at low CF implies that the GEMS might underestimate the GEMS CF value, as measurement pixels with true CFs should be small. An underestimated GEMS CF may lead to an increase in AMF and eventually to the underestimation of NO_2 VCD in the pixels. Further investigation is required to identify the relationship between the GEMS CF and the negative bias tendency of the GEMS NO_2 VCD in less cloudy conditions.

https://doi.org/10.5194/amt-2023-11
Preprint. Discussion started: 8 March 2023

Atmospheric Measurement Techniques Discussions

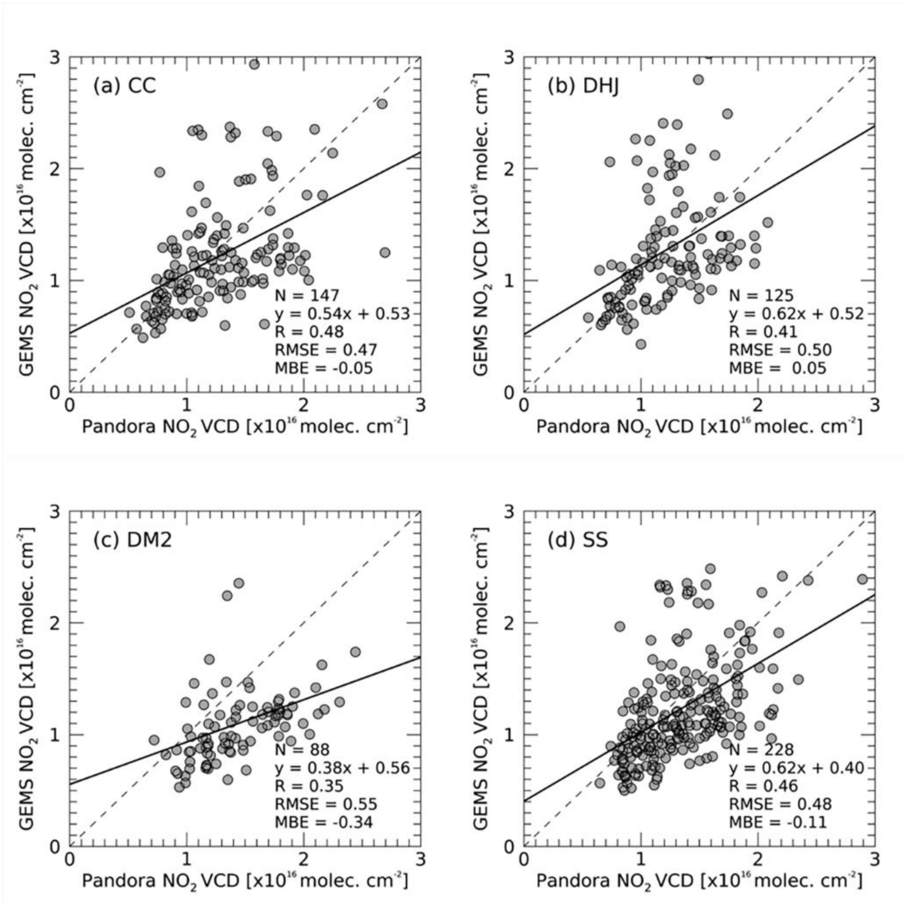

Figure 9. The scatterplot of NO_2 VCD between Pandora and GEMS in the CF conditions < 0.7. (a), (b), (c) and (d) represent the CC, DHJ, DM2, and SS site, respectively. The grey dashed line represents the 1:1 line and the black solid line represents the regression line.

4.3 Correction of horizontal representativeness

The GEMS pixel closest to the Pandora instrument location was used to assess the correlation between Pandora and GEMS NO_2 VCD in Figs 7–9. GEMS does not always observe the same measurement geometry, and the location of each GEMS pixel varies depending on the measurement schedule. The GEMS pixel close to a location where Pandora is installed does not match completely the Pandora observation coverage, so there is a difference occurs between their spatial coverages. In particular, the NO_2 dSCD of Pandora is obtained from an absorption light path between Sun and the instrument at the surface. It is likely that the photons on a light path between Sun and Pandora are absorbed and scattered by both the NO_2 molecules at the lower troposphere in a pixel of the Pandora location and those at rather higher troposphere and stratosphere in the adjoining GEMS pixels, which are located on an azimuth angle connecting Sun and Pandora. Thus, we have attempted to account for the horizontal representativeness of the Pandora observation. First, we selected two pixels of GEMS; one closest pixel to the

https://doi.org/10.5194/amt-2023-11
Preprint. Discussion started: 8 March 2023

Pandora site and another pixel closest to the line of sight (i.e., closest to the viewing azimuth angle of the Pandora measurements). Here we assumed that most of the NO_2 is vertically distributed below 2 km altitude based on the airborne in-situ NO_2 measurements. The weighted mean values of the GEMS NO_2 accounting for the horizontal representativeness are calculated as follows:

$$\mathrm{VCD_{hr}} = \frac{d_2\mathrm{VCD_1} + d_1\mathrm{VCD_2}}{d_1 + d_2},$$

where $\mathrm{VCD_{hr}}$ is the NO_2 VCD accounting for the horizontal representativeness, the d_1 and d_2 are the distances between the Pandora and center of the two GEMS pixels (1 denotes the closest pixel and 2 denotes the pixel to the line of sight), and $\mathrm{VCD_1}$ and $\mathrm{VCD_2}$ are the GEMS NO_2 VCD of the two pixels.

Figure 11 shows the correlations between NO_2 VCD from Pandora and GEMS data which were corrected for the horizontal representativeness of Pandora at CF < 0.3. The correlation coefficients are found 0.69–0.81, which are higher than those without the correction of the horizontal representativeness; the R values at the CC, DHJ, DM2, and SS sites were 0.70, 0.69, 0.81, and 0.75, respectively. Correlations at two sites CC and DM2 are increased with the horizontal representativeness relative to those without the correction, whereas at the DHJ and SS site were similar with or without the correction. RMSEs were 0.37, 0.32, 0.49, and 0.36 with the correction, generally lower than 0.40, 0.33, 0.50, and 0.36 without the correction at the CC, DHJ, DM2, and SS sites, respectively. MBEs with the correction were similar to those without, with values of -0.18, -0.16, -0.43, and -0.2, at the CC, DHJ, DM2, and SS sites, respectively. The variability of Pandora NO_2 VCD with location at a single GEMS pixel has not been investigated in Seosan. However, as shown by the diurnal NO_2 characteristics at the four sites, NO_2 VCD are likely to vary depending on the instrument location at a single GEMS pixel, causing the inherent discrepancies between the GEMS and Pandora.The correction of horizontal representativeness may thus partly account for discrepancies between horizontal and vertical measurement coverages of Pandora and GEMS. Overall, better GEMS–Pandora correlation and lower RMSEs were achieved using the correction for horizontal representativeness.

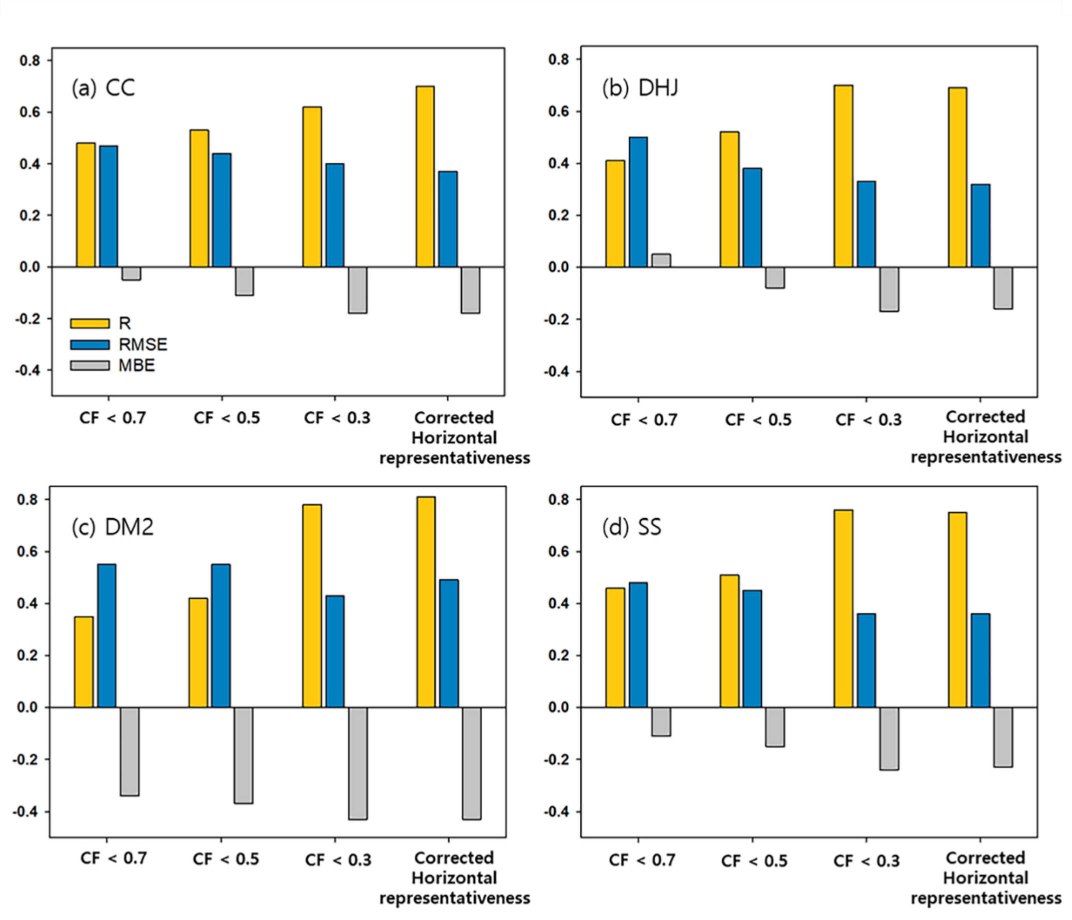

Figure 10. R, RMSE, and MBE between NO_2 VCDs obtained from Pandora and GEMS depending on the CF conditions at (a), (b), (c) and
295 (d) represents CC, DHJ, DM2, and SS site, respectively.

https://doi.org/10.5194/amt-2023-11
Preprint. Discussion started: 8 March 2023

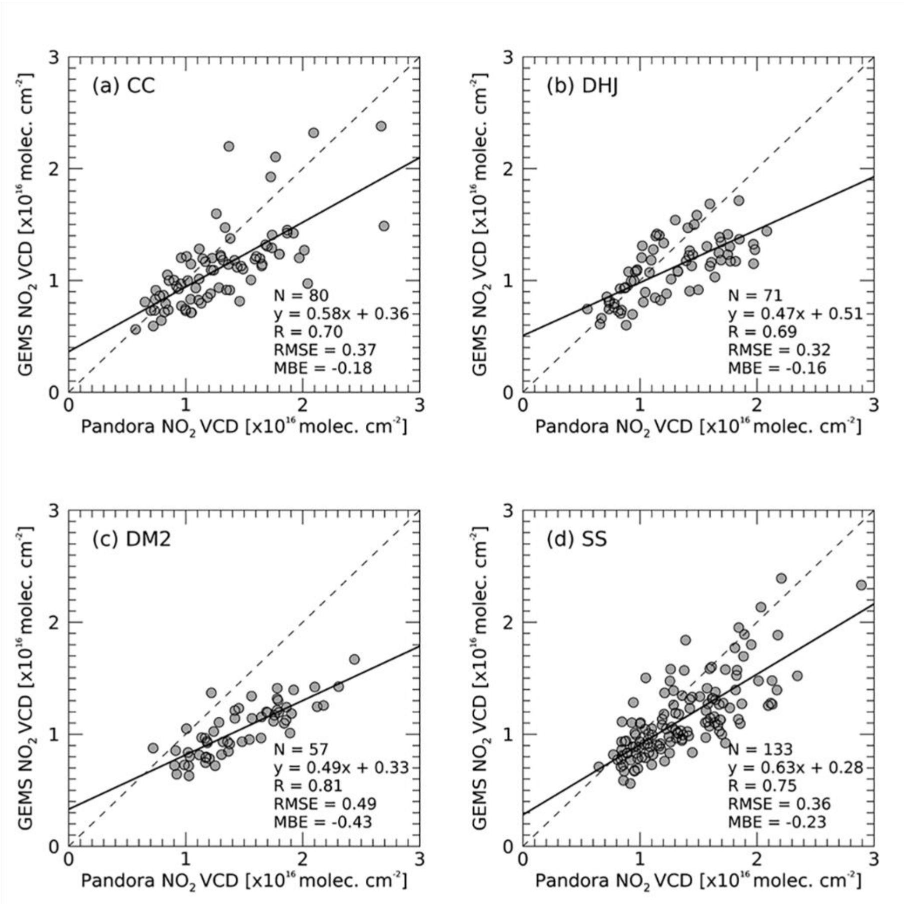

Figure 11. The scatterplot of NO_2 VCD between Pandora and GEMS with the correction for the horizontal representativeness. (a), (b), (c) and (d) represent the CC, DHJ, DM2, and SS site, respectively. The grey dashed line represents the 1:1 line and the black solid line represents the regression line.

5. Conclusion

A first evaluation of GEMS NO_2 carried out via comparison with the NO_2 data obtained from the ground-based Pandora measurement at four sites in Seosan, Korea. An intercomparison of NO_2 VCD among the four Pandora instruments revealed slightly decreasing agreement among instruments with increasing CF, which could contribute partly to an inherent discrepancy between the GEMS and Pandora systems at high CF. It was observed that the correlations of the GEMS NO_2 shows a good agreement against those of Pandora in a less cloudy condition (CF $<$ 0.3). Higher correlation coefficient and lower RMSE were observed at lower CF condition, indicating the higher sensitivity of GEMS to hourly variations in atmospheric NO_2 concentrations under less-cloudy conditions. We also have attempted to account for horizontal representativeness of the

https://doi.org/10.5194/amt-2023-11
Preprint. Discussion started: 8 March 2023

Pandora observation. Mean correlations at the four sites increased with correction for horizontal representativeness, with maximum correlation (R = 0.81) and minimum correlation (R = 0.69) at the DM2 and DHJ sites, respectively. Variation of the correlations between sites may be attribute to variability of the NO_2 VCD observed by Pandora depending on the instrument located at a single GEMS pixel.

Author contributions. DK and SK retrieved and analyzed NO_2 VCDs from Pandora and designed the study, while participating in the campaign. HH, LC, HL, Deok-rae K, Donghee K, JY, DL, UJ, WC and KL planned, organized and performed the Seosan campaign. UJ, CS, SK, SP, JK, and TFH provided and supported instrument management. JK and JP provided GEMS NO_2 data and supported the validation process. All authors reviewed and discussed this paper.

Competing interests. The authors declare that they have no conflict of interest.

References

Bechle, M. J., Millet, D. B., and Marshall, J. D.: Remote sensing of exposure to NO2, satellite versus ground-based measurement in a large urban, Atmos. Environ., 69, 345–353, https://doi.org/10.1016/j.atmosenv.2012.11.046, 2013.

Boersma, K. F., Jacob, D. J., Trainic, M., Rudich, Y., DeSmedt, I., Dirksen, R., and Eskes, H. J.: Validation of urban NO2 concentrations and their diurnal and seasonal variations observed from the SCIAMACHY and OMI sensors using in situ surface measurements in Israeli cities, Atmos. Chem. Phys., 9, 3867–3879, https://doi.org/10.5194/acp-9-3867-2009, 2009

Bovensmann, H., Burrows, J. P., Buchwitz, M., Frerick, J., Noël, S., Rozanov, V. V., Chance, K. V., and Goede, A. P. H.: SCIAMACHY: Mission objectives and measurement modes, J. Atmos. Sci., 56, 127–150, https://doi.org/10.1175/1520-0469(1999)056<0127:SMOAMM>2.0.CO;2, 1999.

Burrows, J., Weber, M., Buchwitz, M., Rozanov, V., LadstatterWeißenmayer, A., Richter, A., Debeek, R., Hoogen, R., Bramstedt, K., Eichmann, K.-U., and Eisinger, M.: The Global Ozone Monitoring Experiment (GOME): Mission concept and first scientific results, J. Atmos. Sci., 56, 151–175, https://doi.org/10.1175/1520-0469(1999)056<0151:TGOMEG>2.0.CO;2, 1999.

Cede, A., Mueller, M., Tiefengraber, M., Abuhassan, N., and Williams, D.: Evaluating the impact of spatial resolution on tropospheric NO2 column comparisons within urban areas using highresolution airborne data, Atmos. Meas. Tech., 12, 6091–6111, https://doi.org/10.5194/amt-12-6091-2019, 2019.

Crutzen, Paul J.: The role of NO and NO2 in the chemistry of the troposphere and stratosphere, Annu. Rev. Earth Planet. Sci., 7, 443-472, https://doi.org/10.1146/annurev.ea.07.050179.002303, 1979.

Fayt, C., De Smedt, I., Letocart, V., Merlaud, A., Pinardi, G., and Van Roozendael, M.: QDOAS Software user manual, available at: https://uv-vis.aeronomie.be/software/QDOAS/QDOAS_manual.pdf (last access: 24 March 2022), 2011.

https://doi.org/10.5194/amt-2023-11
Preprint. Discussion started: 8 March 2023

Atmospheric Measurement Techniques Discussions

Herman, J. R., Cede, A., Spine, E., Mount, G., Tzortziou, M., and Abuhassan, N.: NO2 column amounts from ground-based Pandora and MFDOAS spectrometers using the direct-sun DOAS technique: Intercomparisons and application to OMI validation, J. Geophys. Res., 114, D13307, https://doi.org/10.1029/2009JD011848, 2009.

Herman, J., Spinei, E., Fried, A., Kim, J., Kim, J., Kim, W., Cede, A., Abuhassan, N., and Segal-Rozenhaimer, M.: NO2 and HCHO measurements in Korea from 2012 to 2016 from Pandora spectrometer instruments compared with OMI retrievals and with aircraft measurements during the KORUS-AQ campaign, Atmos. Meas. Tech., 11, 4583–4603, https://doi.org/10.5194/amt-11-4583-2018, 2018.

Herman, J., Abuhassan, N., Kim, J., Kim, J., Dubey, M., Raponi, M., and Tzortziou, M.: Underestimation of column NO2 amounts from the OMI satellite compared to diurnally varying ground-based retrievals from multiple PANDORA spectrometer instruments, Atmos. Meas. Tech., 12, 5593–5612, https://doi.org/10.5194/amt-12-5593-2019, 2019.

Hong, H., Lee, H., Kim, J., Jeong, U., Ryu, J., Lee, D. S.: Investigation of Simultaneous Effects of Aerosol Properties and Aerosol Peak Height on the Air Mass Factors for Space-Borne NO2 Retrievals, Remote Sens., 9, 208, https://doi.org/10.3390/rs9030208, 2017.

Honninger, G., von Friedeburg, C., and Platt, U.: Multi axis differential optical absorption spectroscopy (MAX-DOAS), Atmos.Chem. Phys., 4, 231–254, 2004.

Irie, H., Kanaya, Y., Akimoto, H., Iwabuchi, H., Shimizu, A., and Aoki, K.: First retrieval of tropospheric aerosol profiles using MAX-DOAS and comparison with lidar and sky radiometer measurements, Atmos. Chem. Phys., 8, 341–350, https://doi.org/10.5194/acp-8-341-2008, 2008.

Jeong, U., Hong, H.: Assessment of Tropospheric Concentrations of NO2 from the TROPOMI/Sentinel-5 Precursor for the Estimation of Long-Term Exposure to Surface NO2 over South Korea, Remote Sens. 13 1877, https://doi.org/10.3390/rs13101877, 2021.

Judd, L. M., Al-Saadi, J. A., Janz, S. J., Kowalewski, M. G., Pierce, R. B., Szykman, J. J., Valin, L. C., Swap, R., Cede, A., Mueller, M., Tiefengraber, M., Abuhassan, N., and Williams, D.: Evaluating the impact of spatial resolution on tropospheric NO2 column comparisons within urban areas using highresolution airborne data, Atmos. Meas. Tech., 12, 6091–6111, https://doi.org/10.5194/amt-12-6091-2019, 2019.

Judd, L. M., Al-Saadi, J. A., Szykman, J. J., Valin, L. C., Janz, S. J., Kowalewski, M. G., Eskes, H. J., Veefkind, J. P., Cede, A., Mueller, M., Gebetsberger, M., Swap, R., Pierce, R. B., Nowlan, C. R., Abad, G. G., Nehrir, A., and Williams, D.: Evaluating Sentinel-5P TROPOMI tropospheric NO2 column densities with airborne and Pandora spectrometers near New York City and Long Island Sound, Atmos. Meas. Tech., 13, 6113–6140, https://doi.org/10.5194/amt-13-6113-2020, 2020.

Kim, J., Jeong, U., Ahn, M.-H., Kim, J. H., Park, R. J., Lee, H., Song, C. H., Choi, Y.-S., Lee, K.-H., Yoo, J.-M., Jeong, M.-J., Park, S. K., Lee, K.-M., Song, C.-K., Kim, S.-W., Kim, Y. J., Kim, S.-W., Kim, M., Go, S., Liu, X., Chance, K., Miller, C. C., Al-Saadi, J., Veihelmann, B., Bhartia, P. K., Torres, O., Abad, G. G., Haffner, D. P., Ko, D. H., Lee, S. H., Woo, J.-H., Chong, H., Park, S. S., Nicks, D., Choi, W. J., Moon, K.-J., Cho, A., Yoon, J., Kim, S.-K., Hong, H., Lee, K., Lee, H., Lee, S., Choi, M., Veefkind, P., Levelt, P. F., Edwards, D. P., Kang, M., Eo, M., Bak, J., Baek, K., Kwon, H.-A., Yang, J., Park, J., Han, K. M., Kim, B.-R., Shin, H.-W., Choi, H., Lee, E., Chong, J., Cha, Y., Koo, J.-H., Irie, H., Hayashida, S., Kasai, Y., Kanaya, Y., Liu, C., Lin, J., Crawford, J. H., Carmichael, G. R., Newchurch, M. J., Lefer, B. L., Herman, J. R., Swap, R. J., Lau, A. K. H., Kurosu, T. P., Jaross, G., Ahlers, B., Dobber, M., McElroy, C. T., and Choi, Y.: New era of air quality monitoring from space, Geostationary Environment Monitoring Spectrometer (GEMS), B. Am. Meteorol. Soc., 101, E1–E22, https://doi.org/10.1175/BAMS-D-18-0013.1, 2020.

Lamsal, L. N., Krotkov, N. A., Celarier, E. A., Swartz, W. H., Pickering, K. E., Bucsela, E. J., Gleason, J. F., Martin, R. V., Philip, S., Irie, H., Cede, A., Herman, J., Weinheimer, A., Szykman, J. J., and Knepp, T. N.: Evaluation of OMI operational standard NO2 column retrievals using in situ and surface-based NO2 observations, Atmos. Chem. Phys., 14, 11587–11609, https://doi.org/10.5194/acp-14-11587-2014, 2014.

Levelt, P. F., Hilsenrath, E., Leppelmeier, G. W., van den Oord, G. B. J., Bhartia, P. K., Tamminen, J., de Haan, J. F., and Veefkind, J. P.: Science Objectives of the Ozone Monitoring Instrument, IEEE T. Geosci. Remote, 44, 1199–1208, https://doi.org/10.1109/TGRS.2006.872333, 2006.

Munro, R., Lang, R., Klaes, D., Poli, G., Retscher, C., Lindstrot, R., Huckle, R., Lacan, A., Grzegorski, M., Holdak, A., Kokhanovsky, A., Livschitz, J., and Eisinger, M.: The GOME2 instrument on the Metop series of satellites: instrument design, calibration, and level 1 data processing – an overview, Atmos. Meas. Tech., 9, 1279–1301, https://doi.org/10.5194/amt-9-1279-2016, 2016.

Park, J., Lee, H., Hong, H.: Geostationary Environment Monitoring Spectrometer (GEMS) Algorithm Theoretical Basis Document NO2 Retrieval Algorithm, available at: https://nesc.nier.go.kr/product/document?page=1&limit=10, (last access: 24 March 2022), 2020.

Pinardi, G., Van Roozendael, M., Hendrick, F., Theys, N., Abuhassan, N., Bais, A., Boersma, F., Cede, A., Chong, J., Donner, S., Drosoglou, T., Dzhola, A., Eskes, H., Frieß, U., Granville, J., Herman, J. R., Holla, R., Hovila, J., Irie, H., Kanaya, Y., Karagkiozidis, D., Kouremeti, N., Lambert, J.-C., Ma, J., Peters, E., Piters, A., Postylyakov, O., Richter, A., Remmers, J., Takashima, H., Tiefengraber, M., Valks, P., Vlemmix, T., Wagner, T., and Wittrock, F.: Validation of tropospheric NO2 column measurements of GOME-2A and OMI using MAX-DOAS and direct sun network observations, Atmos. Meas. Tech., 13, 6141–6174, https://doi.org/10.5194/amt-13-6141-2020, 2020.

Seinfeld, J. H. and Pandis, S. N.: Atmospheric Chemistry and Physics: From Air Pollution to Climate Change, John Wiley & Sons, Inc., 1998.

Serdyuchenko, A., Gorshelev, V., Weber, M., Chehade, W., and Burrows, J. P.: High spectral resolution ozone absorption cross-sections – Part 2: Temperature dependence, Atmos. Meas. Tech.,7, 625–636, https://doi.org/10.5194/amt-7-625-2014, 2014.

Thalman, R. and Volkamer, R.: Temperature dependant absorption cross-sections of O2−O2 collision pairs between 340 and 630 nm at atmospherically relevant pressure Phys. Chem. Chem. Phys., 15, 15371–15381, doi: 10.1039/C3CP50968K, 2013.

https://doi.org/10.5194/amt-2023-11
Preprint. Discussion started: 8 March 2023

Tzortziou, M., Herman, J. R., Ahmad, Z., Loughner, C. P., Abuhassan, N., and Cede, A.: Atmospheric NO2 dynamics and impact on ocean color retrievals in urban nearshore regions, J. Geophys. Res.-Oceans, 119, 3834–3854, https://doi.org/10.1002/2014JC009803, 2014.

Tzortziou, M., Herman, J. R., Cede, A., Loughner, C. P., Abuhassan, N., and Naik, S.: Spatial and temporal variability of ozone and nitrogen dioxide over a major urban estuarine ecosystem, J. Atmos. Chem., 72, 287–309, https://doi.org/10.1007/s10874-013-9255-8, 2015.

Vandaele, A., Hermans, C., Simon, P., Carleer, M., Colin, R., Fally, S., M'erienne, M., Jenouvrier, A., and Coquart, B.: Measurements of the NO2 absorption cross-section from 42 000 cm−1 to 10 000 cm−1 (238–1000 nm) at 220 K and 294 K, J. Quant. Spectrosc. Ra., 59, 171–184, https://doi.org/10.1016/s0022-4073(97)00168-4, 1998.

Veefkind, J. P., Aben, I., McMullan, K., Förster, H., de Vries, M., Otter, G., Claas, J., Eskes, H. J., de Haan, J. F., Kleipool, Q.L., van Weele, M., Hasekamp, O., Hoogeveen, R., Landgraf, J., Snel, R., Tol, P., Ingmann, P., Voors, R., Kruizinga, B., Vink, R., Visser, H., Levelt, P. F., and de Vries, J.: TROPOMI on the ESA Sentinel-5 Precursor: A GMES mission for global observations of the atmospheric composition for climate, air quality and ozone layer applications, Remote Sens. Environ., 120, 70–83 https://doi.org/10.5194/amt-13-6113-2020, 2012.

Verhoelst, T., Compernolle, S., Pinardi, G., Lambert, J.-C., Eskes, H. J., Eichmann, K.-U., Fjæraa, A. M., Granville, J., Niemeijer, S., Cede, A., Tiefengraber, M., Hendrick, F., Pazmiño, A., Bais, A., Bazureau, A., Boersma, K. F., Bognar, K., Dehn, A., Donner, S., Elokhov, A., Gebetsberger, M., Goutail, F., Grutter de la Mora, M., Gruzdev, A., Gratsea, M., Hansen, G. H., Irie, H., Jepsen, N., Kanaya, Y., Karagkiozidis, D., Kivi, R., Kreher, K., Levelt, P. F., Liu, C., Müller, M., Navarro Comas, M., Piters, A. J. M., Pommereau, J.-P., Portafaix, T., Prados-Roman, C., Puentedura, O., Querel, R., Remmers, J., Richter, A., Rimmer, J., Rivera Cárdenas, C., Saavedra de Miguel, L., Sinyakov, V. P., Stremme, W., Strong, K., Van Roozendael, M., Veefkind, J. P., Wagner, T., Wittrock, F., Yela González, M., and Zehner, C.: Ground-based validation of the Copernicus Sentinel-5P TROPOMI NO2 measurements with the NDACC ZSL-DOAS, MAX-DOAS and Pandonia global networks, Atmos. Meas. Tech., 14, 481–510, https://doi.org/10.5194/amt-14-481-2021, 2021.

Wagner, T., Beirle, S., Brauers, T., Deutschmann, T., Frieß, U., Hak, C., Halla, J. D., Heue, K. P., Junkermann, W., Li, X., Platt, U., and Pundt-Gruber, I.: Inversion of tropospheric profiles of aerosol extinction and HCHO and NO2 mixing ratios from MAX-DOAS observations in Milano during the summer of 2003 and comparison with independent data sets, Atmos. Meas. Tech., 4, 2685–2715, https://doi.org/10.5194/amt-4-2685-2011, 2011.

Wang, Y., Beirle, S., Lampel, J., Koukouli, M., De Smedt, I., Theys, N., Li, A., Wu, D., Xie, P., Liu, C., Van Roozendael, M., Stavrakou, T., Müller, J.-F., and Wagner, T.: Validation of OMI, GOME-2A and GOME-2B tropospheric NO2, SO2 and HCHO products using MAX-DOAS observations from 2011 to 2014 in Wuxi, China: investigation of the effects of priori profiles and aerosols on the satellite products, Atmos. Chem. Phys., 17, 5007–5033, https://doi.org/10.5194/acp-17-5007-2017, 2017.